TITLE:

Magnetotransport study of the canted antiferromagnetic phase in bilayer nu=2 quantum Hall state

AUTHOR(S):

Fukuda, A; Sawada, A; Kozumi, S; Terasawa, D; Shimoda, Y; Ezawa, ZF; Kumada, N; Hirayama, Y

CITATION:

Fukuda, A ...[et al]. Magnetotransport study of the canted antiferromagnetic phase in bilayer nu=2 quantum Hall state. PHYSICAL REVIEW B 2006, 73(16): 165304.

ISSUE DATE:

2006-04

URL:

http://hdl.handle.net/2433/50512

RIGHT:

Copyright 2006 American Physical Society

京都大学学術情報リポジトリ
KURENAI
Kyoto University Research Information Repository

京都大学 KYOTO UNIVERSITY
A Self-archived copy in
Kyoto University Research Information Repository
https://repository.kulib.kyoto-u.ac.jp
京都大学学術情報リポジトリ KURENAI 紅 Kyoto University Research Information Repository

PHYSICAL REVIEW B **73**, 165304 (2006)

Magnetotransport study of the canted antiferromagnetic phase in bilayer $\nu=2$ quantum Hall state

A. Fukuda* and A. Sawada
Research Center for Low Temperature and Materials Sciences, Kyoto University, Kyoto 606-8502, Japan

S. Kozumi, D. Terasawa, Y. Shimoda, and Z. F. Ezawa
Graduate School of Science, Department of Physics, Tohoku University, Sendai 980-8578, Japan

N. Kumada and Y. Hirayama
NTT Basic Research Laboratories, NTT Corporations, 3-1 Morinosato-Wakamiya, Atsugi 243-0198, Japan
(Received 28 December 2005; published 3 April 2006)

Magnetotransport properties are investigated in the bilayer quantum Hall state at the total filling factor $\nu=2$. We measured the activation energy elaborately as a function of the total electron density and the density difference between the two layers. Our experimental data demonstrate clearly the emergence of the canted antiferromagnetic (CAF) phase between the ferromagnetic phase and the spin-singlet phase. The stability of the CAF phase is discussed by the comparison between experimental results and theoretical calculations using a Hartree-Fock approximation and an exact diagonalization study. The data reveal also an intrinsic structure of the CAF phase divided into two regions according to the dominancy between the intralayer and interlayer correlations.

DOI: 10.1103/PhysRevB.73.165304 PACS number(s): 73.43.Nq, 73.43.Qt

I. INTRODUCTION

Two-dimensional electron gas provides us with a simplest low-dimensional condensed matter system having the spin degree of freedom. It has a conceptual link to the unconventional superconductivities,[1] Bose-Einstein condensation in two dimensions[2,3] and superfluidity of ^{3}He film.[4] However, more fascinating phenomena are anticipated by introducing an additional degree of freedom to the two-dimensional electron systems.

In the last decade, many efforts were devoted to study bilayer quantum Hall (QH) systems,[5,6] which have an additional layer degree of freedom associated with the third dimension. The layer degree of freedom is regarded as a virtual one-half spin system and named "pseudospin." Although the total filling factor $\nu=1$ QH system has only one phase without in-plane magnetic field, the $\nu=2$ QH system has a variety of quantum phases related to a combination of the spin and the pseudospin. At $\nu=2$, in a naive one-body picture, a phase transition occurs because of the competition between the tunneling energy Δ_{SAS} and the Zeeman energy Δ_Z. As a result, two phases occur: one is the spin-ferromagnet and pseudospin-singlet phase (F phase) for $\Delta_{SAS}<\Delta_Z$ and the other is the spin-singlet and pseudospin-ferromagnet phase (S phase) for $\Delta_{SAS}>\Delta_Z$. The F phase consists of two single-layer $\nu=1$ QH systems. The S phase has an interlayer phase coherence due to the interlayer Coulomb interaction. Between these two phases, a novel canted antiferromagnet phase (CAF phase) has been argued to emerge.[7,8]

The first experimental indication of a new phase in the $\nu=2$ bilayer QH system was given by inelastic light scattering spectroscopy by Pelligrini *et al.*[9] They also observed mode softening signals indicating second-order phase transitions.[10] The new phase was theoretically identified as the CAF phase by Das Sarma *et al.*[7,8] They obtained the phase diagram in the Δ_{SAS}-d plane based on a time-dependent Hartree-Fock (HF) analysis, where d is the layer separation. An effective spin theory,[11,12] a Hartree-Fock-Bogoliubov approximation[13] and an exact diagonalization (ED) study[14] followed to improve the phase diagram by more precise calculations. Effects of the density imbalance on the CAF phase were also discussed and several different phases are expected to emerge.[15,16] Recently the phase diagram in the σ-n_T plane was constructed,[17] where n_T is the total electron density and σ is the density imbalance between the two layers. Though capacitance spectroscopy[18] as well as magnetotransport measurements[19–22] were carried out, experimental studies on the CAF phase remain less systematic than theoretical works.

This paper is organized as follows. In Sec. II our experimental setup is described. In Sec. III we report the results of elaborate magnetotransport experiments performed to quest for essential features of the CAF phase. Activation energy measurements as a function of n_T and σ show clearly that there exist three phases to be identified as the F, S, and CAF phases. In Sec. IV we present the phase diagram in the σ-n_T plane. We have demonstrated that the layer density imbalance causes new quantum states, i.e., two regions in the CAF phase, which have never been predicted theoretically. We also try to figure out the intrinsic spin and pseudospin structures of new regions. In Sec. V the phase diagram of the $\nu=2$ bilayer QH system in the n_T-Δ_{SAS} plane is presented. Theoretical considerations by the HF approximation and the ED study are made. The ED analysis gives a quantitative support to the emergence of the CAF phase. In Sec. VI, we comment on the comparison between our results and several theoretical works.

 ©2006 The American Physical Society

京都大学 KYOTO UNIVERSITY
A Self-archived copy in
Kyoto University Research Information Repository
https://repository.kulib.kyoto-u.ac.jp
京都大学学術情報リポジトリ KURENAI 紅 Kyoto University Research Information Repository

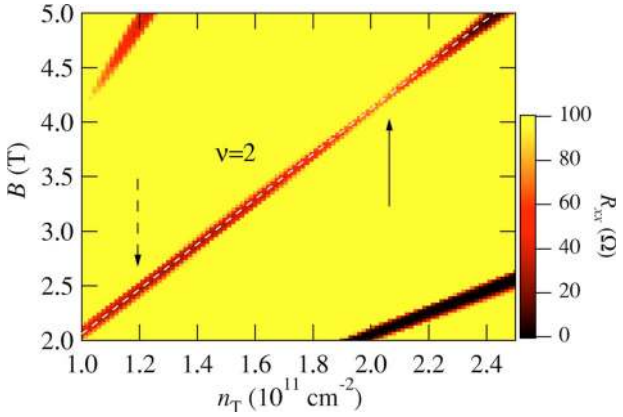

FIG. 1. (Color online) Image plot of the magnetoresistance R_{xx} around the $\nu=2$ QH state as a function of the total density n_T and the magnetic field B at a temperature of 1.11 K. The white dashed line is located just on the $\nu=2$ filling.

II. EXPERIMENTS

We used a sample consisting of two GaAs quantum wells of 20 nm in width separated by a 3.1-nm-thick $Al_{0.33}Ga_{0.67}As$ barrier. The sample was grown by molecular-beam epitaxy. Si-modulation doping is carried out only on the front side of the double-quantum-well (DQW) structure and electrons in the back side of the DQW is fully field induced by applying a positive bias to the underlying n^+-GaAs gate.[23] The tunneling energy Δ_{SAS} is 11 K, the layer separation d is 23.1 nm, and the low-temperature mobility at $n_T=1.0\times10^{11}$ cm^{-2} is 1.0×10^6 cm^2/V s. We can control n_T up to 3.0×10^{11} cm^{-2} and the density imbalance parameter σ from 0 at the balanced configuration to ±1 at the monolayer configuration continuously by applying the front- and back-gate voltages. The density imbalance parameter is defined by $\sigma\equiv(n_f-n_b)/(n_f+n_b)$, where n_f (n_b) is the electron density in the front (back) layer. To measure resistances, standard low-frequency ac lock-in techniques were used with a current of 20 nA and a frequency of 16.6 Hz. Throughout measurements, magnetic field is applied perpendicular to the two-dimensional plane.

III. ACTIVATION ENERGY MEASUREMENTS

First, we investigate the bilayer $\nu=2$ QH states in the balanced density configuration ($\sigma=0$). Figure 1 shows R_{xx} as a function of the magnetic field B and n_T, where n_T is scanned while keeping $n_f=n_b$. Dark regions represent smaller R_{xx} and thus QH states. The central black region around the white dashed line running from lower left to upper right in the figure indicates the $\nu=2$ QH state. The width of the black region is related to the stability of the QH state. With increasing n_T, the width increases to the point indicated by the dashed arrow in Fig. 1, then decreases to the one indicated by the solid arrow, and increases again. This implies that the $\nu=2$ QH state becomes stable, then less stable and stable again as a function of n_T.

To clarify this fact more, we measured the n_T dependence of the activation energy Δ, which was determined from the

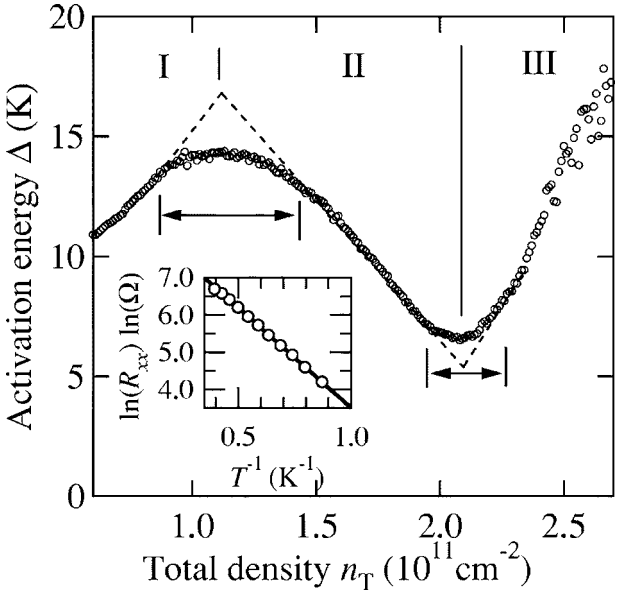

FIG. 2. Activation energy Δ as a function of the total density n_T in the balanced configuration. Three different regions are found and labeled I, II, and III. See details in the text. Inset: Arrehnius plot of the magnetoresistance R_{xx} at $n_T=1.66\times10^{11}$ cm^{-2}.

slope of the Arrehnius plot of the longitudinal resistance R_{xx}, $R_{xx}=R_0\exp(-\Delta/2T)$, where T is the temperature. Figure 2 shows the activation energy as a function of n_T in the balanced configuration ($\sigma=0$). In the beginning, Δ gradually increases for the increment of n_T from 0.6×10^{11} to 1.1×10^{11} cm^{-2}. After crossing the maximum, Δ decreases to the minimum at $n_T=2.1\times10^{11}$ cm^{-2}. Finally, Δ steeply increases after crossing the minimum point. This figure indicates that there are, at least, three phases in the balanced configuration in the $\nu=2$ QH state. We named them the phases I, II, and III from the low n_T to high n_T region as in Fig. 2. According to a number of theories mentioned above, the phases I, II, and III should correspond to the S, CAF, and F phases, respectively. It should be noted that Δ changes smoothly from the region I to II, and from II to III. This indicates that both phase transitions are not first order, as agrees well with the theoretical results.[7,8,17] It is also consistent with the light-scattering experimental result.[10] Although the exact phase transition point is not clear because of the smooth change, it would exist around n_T that gives the local maximum or minimum, probably in the range shown as the two-headed arrows in Fig. 2. Hereafter we adopt the point that gives the local maximum or minimum of Δ as a representative phase transition point.

To confirm the identification of these three phases at $\sigma=0$, we also investigated the stability of the $\nu=2$ QH states against the layer density imbalance σ through the magnetotransport measurements in Fig. 3. We present image plots of the magnetoresistance R_{xx} by changing the magnetic field B and the layer density imbalance σ. The black region represents the well-developed $\nu=2$ QH states. We display three typical patterns of R_{xx} for three values of n_T. We remark the following characteristic features of the pattern as $|\sigma|$ is increased. (a) At $n_T=0.8\times10^{11}$ cm^{-2} (region I at $\sigma=0$), the

京都大学 KYOTO UNIVERSITY
A Self-archived copy in
Kyoto University Research Information Repository
https://repository.kulib.kyoto-u.ac.jp
京都大学学術情報リポジトリ KURENAI 紅 Kyoto University Research Information Repository

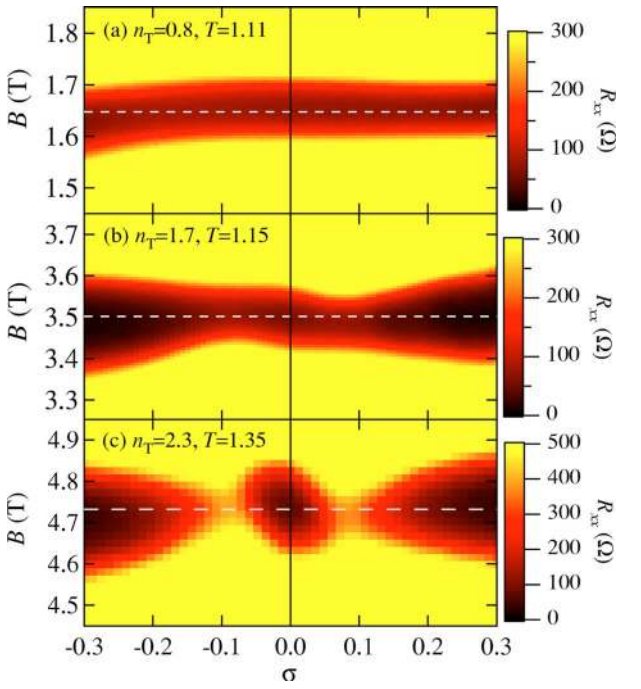

FIG. 3. (Color online) Image plots of the magnetoresistance R_{xx} around the $\nu=2$ QH state as a function of the density imbalance σ and the magnetic field B at the fixed total density n_T. Each n_T (10^{11} cm^{-2}) and temperature (K) are shown in the graph. The solid line indicates $\sigma=0$. The white dashed lines are located just on the $\nu=2$ filling.

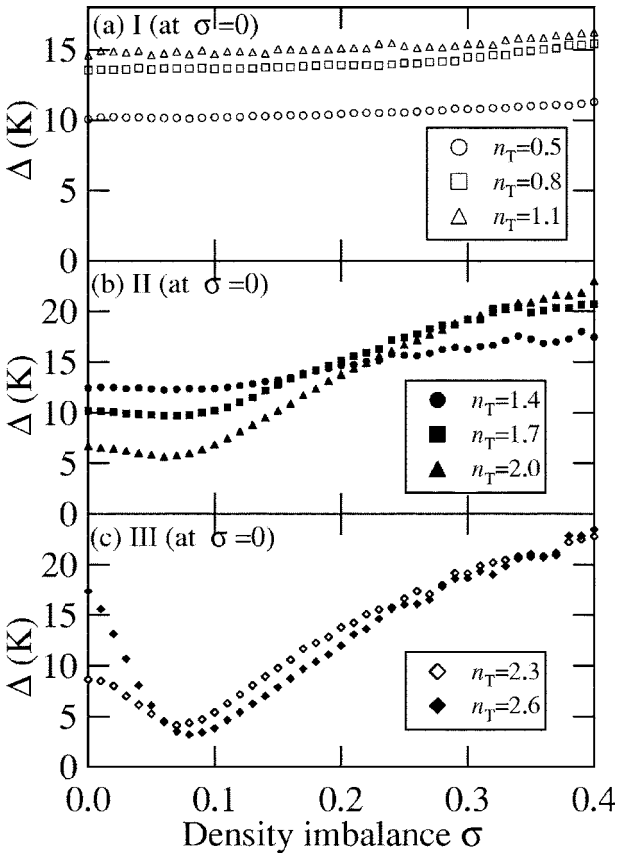

FIG. 4. Activation energy Δ as a function of the density imbalance σ at the fixed total density n_T. Data in (a), (b), and (c) are for n_T in the phase I, II, and III at $\sigma=0$, respectively. The unit of n_T noted in the graphs is $\times 10^{11}$ cm^{-2}.

width of the stable region is almost constant. (b) At $n_T=1.7\times10^{11}$ cm^{-2} (region II at $\sigma=0$), it becomes narrower and then wider slightly. (c) At $n_T=2.3\times10^{11}$ cm^{-2} (region III at $\sigma=0$), it becomes narrower and then wider drastically.

To investigate the stability of these three phases against the density imbalance further, in a similar way we did for n_T, we also carried out the activation energy measurements as a function of σ. Results in each region are shown in Fig. 4. Although the identification of the phase at large density imbalance is important, about which we will discuss later, here we focus on the properties in the vicinity of $\sigma=0$. In phase I, the activation energy Δ is almost constant or gradually increases as σ is increased. It indicates that the phase I at $\sigma=0$ is robust against the density imbalance. This fact supports that the phase I corresponds to the S phase because the S phase is stabilized by the interlayer correlation. On the other hand, in the phase III near $\sigma=0$, Δ steeply decreases for the initial increment of σ. It indicates that the phase III at $\sigma=0$ is feeble against the density imbalance. This fact points out that the phase III accords to the F phase because the F phase consists of two single-layer $\nu=1$ QH states.[19–21] In the phase II, Δ slightly decreases or is almost constant for small density imbalance. Taking account of the dependence of Δ on n_T and σ, the phase II is concluded to have properties quite different from the phases I and III.

IV. PHASE DIAGRAM IN THE σ-n_T PLANE

We next construct the phase diagram in the σ-n_T plane [Fig. 5(b)]. At $\sigma=0$ the CAF-F (S-CAF) phase boundary is given by the local minimum (maximum) of Δ in Fig. 2. We made similar measurements at various values of σ. Several data are displayed in Fig. 5(a). As σ is increased, the n_T that gives the maximum of Δ, the S-CAF phase boundary, stays almost constant when $\sigma<0.1$ and then moves towards the larger n_T side when $\sigma>0.1$. On the other hand, the point that gives the minimum of Δ, the CAF-F phase boundary, shifts to larger n_T for small increase in σ, and disappear when $\sigma>0.1$.

We plot the set of these values (σ,n_T) as open triangles (circles) in Fig. 5(b), which gives the CAF-F (S-CAF) phase boundary. It is found that the experimentally determined F region has a finite width in σ. According to a theoretical work,[17] however, the F phase is only stable just at the balanced point for the ideal case without impurities. The origin of this discrepancy can be attributed to an impurity effect. In the F phase, the $\nu=1$ QH states are formed in both front and back layers. Once impurities broaden the plateau width for each layer, the F phase appears in the overlap region of two $\nu=1$ QH states even if the density imbalance is made between the two layers. This is illustrated in Fig. 6.

We continue to analyze the phase diagram in the σ-n_T plane [Fig. 5(b)]. We now focus on the minimum of Δ in Fig. 4. We extract a set of values (σ,n_T) that gives the minimum of Δ, which are drawn as open diamonds in the phase diagram. It is interesting that the boundary (open diamonds)

京都大学 KYOTO UNIVERSITY
A Self-archived copy in
Kyoto University Research Information Repository
https://repository.kulib.kyoto-u.ac.jp
京都大学学術情報リポジトリ KURENAI 紅 Kyoto University Research Information Repository

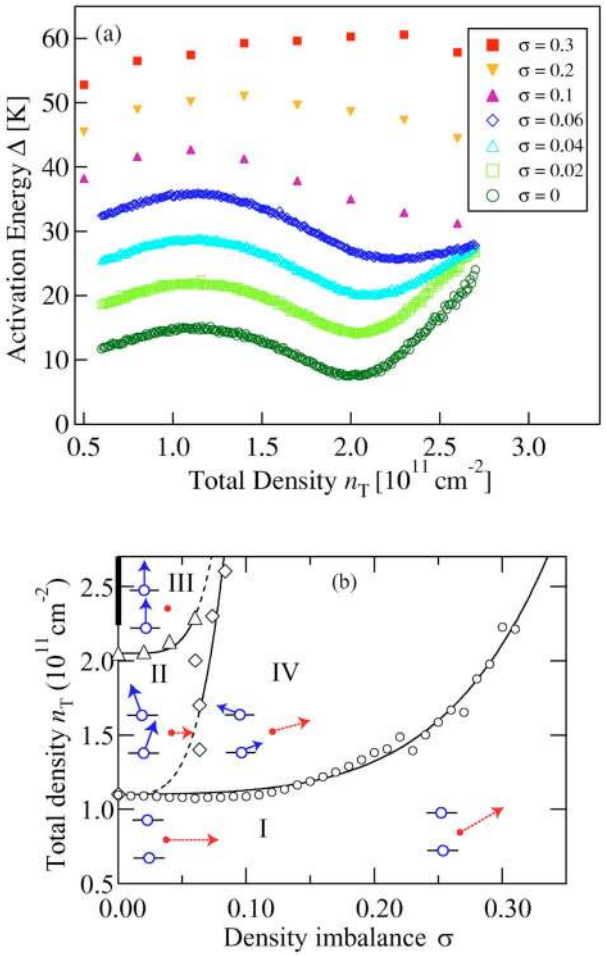

FIG. 5. (Color online) (a) Activation energy Δ as a function of the total density n_T for several density imbalance σ. The σ for each data is listed in the graph. The Δ at $\sigma=0$ has a correct scale and each trace for $\sigma\neq 0$ is shifted by 7 K for easy to see. (b) Phase diagram in the σ-n_T plane. Open triangles (circles) are the n_T's that give the local minima (maxima) of the activation energy at fixed σ. The fat solid line just on the vertical axis for $n_T > 2.24 \times 10^{11}$ cm^{-2} is a theoretically predicted F phase, which would be stable only at the balanced point but for an impurity effect. Open diamonds give the II-IV region boundary. Solid lines are guides for eyes for region boundaries and dashed lines represent ambiguous boundaries. The predicted structures of the spin (blue solid arrow) in the front and back layers and the total pseudospin (red dashed arrow) are also illustrated.

does not coincide either with the CAF-F boundary or the CAF-S boundary. It means that there exist two regions shown as II and IV in the CAF phase. The II-IV boundary seems to be smoothly extrapolated to the I-II boundary point at $\sigma=0$ (dashed line) because no minimum was found at $n_T=1.1\times10^{11}$ cm^{-2} in Fig. 4(a).

The identification of the regions II and IV is intriguing. The characteristic features of the activation energy Δ are summarized as follows: As the density imbalance increases, Δ decreases in the region II just as in the F phase, while Δ increases in the region IV just as in the S phase. Recall that the intralayer (interlayer) interaction destabilarizes (stabilarizes) the QH system against the density imbalance. In addition to the CAF phase emerges by the interplay between the spin and pseudospin interactions, that is to say, between intralayer and interlayer interactions. Since it is natural that the behavior of the activation energy is mainly controlled by the dominant interaction, the intralayer (interlayer) interaction is dominant in the region II (IV). Hence we call regions II and IV the F-like CAF (FCAF) and S-like CAF (SCAF), respectively. The experimentally found II-IV region boundary in Fig. 5(b) must represent the balanced point between the interlayer and intralayer correlations in the two-dimensional electron systems.

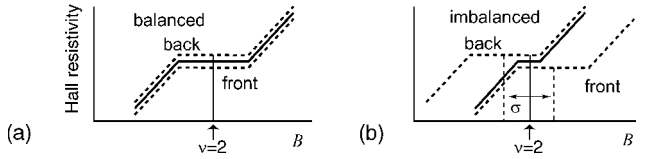

FIG. 6. Illustration of the F phase at $\nu=2$. It consists of two monolayer $\nu=1$ QH states in the front and back layers. (a) At the balanced point, the $\nu=1$ Hall plateau (dotted lines) develops due to impurity effects in each layer, and so does the $\nu=2$ Hall plateau (thick line). (b) At the imbalanced point ($\sigma>0$), the number of electrons is more (less) than the number of flux quanta in the front (back) layer. In the front (back) layer with more (less) electrons, the Hall plateau (dotted line) would be generated with its center being located at a higher (lower) field, as indicated by a dotted vertical line. Then the $\nu=2$ Hall plateau (thick line) is generated in the region where the two $\nu=1$ Hall plateaux (dotted lines) in the front and back layers overlap.

The structure of the spin and pseudospin has been calculated in each phase,[17] which is illustrated in Fig. 5(b). The magnitude of the total spin $|S|$ (the pseudospin $|P|$) is maximal in the F phase (S phase), decreases in the CAF phase and finally vanishes in the S phase (F phase). It is well known[7,8] that the spins are canted and make an antiferromagnetic correlation between the two layers in the CAF phase. The II-IV region boundary would be given when the ratio $|S|/|P|$ takes a certain critical value depending on the tunneling and Zeeman gaps, though its theoretical understanding is yet to be explored. We summarize various properties of each region in Table I.

V. PHASE DIAGRAM IN THE n_T-Δ_{SAS} PLANE

Finally we construct the phase diagram in the n_T-Δ_{SAS} plane. The theoretical S-CAF phase boundary is calculated by the HF approximation from the equation[8,15,17]

TABLE I. Summary of the notation of each phase and its properties against the total density n_T and the density imbalance σ.

Region	I	IV	II	III
Phase	S	SCAF	FCAF	F
$\partial\Delta/\partial n_T$	+	−	−	+
$\partial\Delta/\partial\sigma$	+	+	−	−

京都大学 KYOTO UNIVERSITY
A Self-archived copy in
Kyoto University Research Information Repository
https://repository.kulib.kyoto-u.ac.jp
京都大学学術情報リポジトリ KURENAI 紅 Kyoto University Research Information Repository

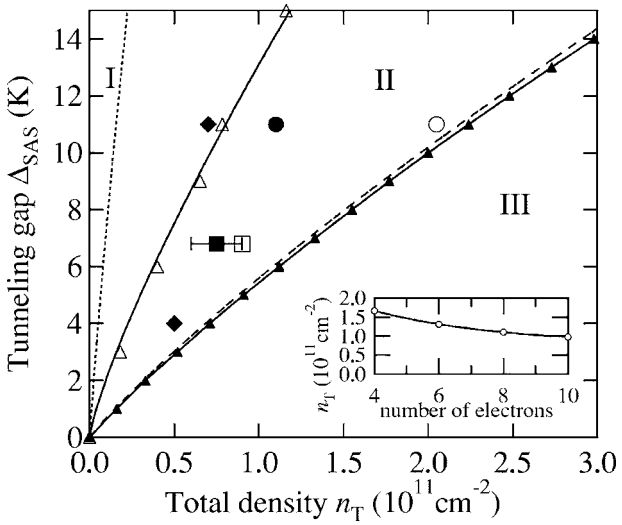

FIG. 7. Phase diagram in the n_T-Δ_{SAS} plane at the balanced point. The solid and open circles are the S(I)-CAF(II) and CAF(II)-F(III) phase transition points derived from the data in Fig. 2, respectively. The open square is a reinterpreted S-CAF phase boundary, while the error bar on the solid square shows that the CAF-F phase boundary must be within this region, as estimated from Ref. 19. The solid diamonds are reinterpreted S-CAF phase boundary determined from the SCAF-FCAF region boundary appeared in Ref. 21. See details in the text. The dotted line and dashed line are the calculated S-CAF and CAF-F phase boundaries by the Hartree-Fock approximation. Open triangles and solid triangles are the calculated S-CAF and CAF-F phase boundary points by an exact diagonalization method. Inset: Convergency of the ED method. The total density n_T at the CAF-F transition point vs the number of electrons to be diagonalized for Δ_{SAS}=11 K.

$$\Delta_Z = \sqrt{\Delta_{SAS}(\Delta_{SAS} - E_C)},$$

where E_C is the capacitance energy between two layers. In the same way, the CAF-F phase boundary is determined from the equation

$$\Delta_Z = \sqrt{\Delta_{SAS}^2 + \left(\frac{E_C}{2}\right)^2} - \frac{E_C}{2}.$$

They are shown in Fig. 7 by the dotted and dashed lines, respectively. However, an ED study has suggested[14] that the S-CAF phase boundary in the HF approximation is not reliable. We carried out an ED analysis of the phase diagram in the n_T-Δ_{SAS} plane, whose results are plotted as open triangles with solid lines in the same figure. The convergency for the CAF-F phase boundary is quite good for more than six particles to be diagonalized. On the other hand, calculated points on the S-CAF boundary converge only gradually against the number of particles N (see the inset in Fig. 7). We display the asymptotic values for $N \to \infty$ in Fig. 7. The agreement of the CAF-F boundary between the HF approximation and the ED analysis is extremely good. This is because the HF result is exact for the CAF-F boundary.[17]

We mark the n_T-Δ_{SAS} phase diagram (Fig. 7) with open and solid circles representing the present experimental results. The agreement of our experimental data points with the ED analysis is reasonably well but not perfect. The disagreement would be due to the finite width of quantum wells, which is neglected in theoretical calculations but is known to modify the Coulomb energy considerably.

Here we review the experimental data given in Ref. 19, where a sample with Δ_{SAS}=6.7 K was used. In view of our present understanding, the phase transition point at n_T=0.9 $\times 10^{11}$ cm^{-2} in Fig. 4 of this reference is interpreted as the CAF-F phase boundary. On the other hand, there is no definite data for the S-CAF phase boundary. Nevertheless, Fig. 3 of this reference tells us that the QH state at n_T=0.6 $\times 10^{11}$ cm^{-2} is in the S phase. Hence, the S-CAF phase boundary must be between 0.6×10^{11} and 0.9×10^{11} cm^{-2}. We plot these points as squares in Fig. 7. We also reanalyzed the data based on Hall-plateau width measurements in Ref. 21. Though they did not find any phase transition points at σ=0 for two samples with Δ_{SAS}=1 K and Δ_{SAS} =23–32 K, they did for two other samples with Δ_{SAS}=4 K and Δ_{SAS}=11 K. They identified the point that gives the minimum of the Hall plateau width for σ at the fixed n_T as the F-S phase transition point. However, from our current understanding, the point which gives the minimum of Δ against σ should be interpreted as the SCAF-FCAF phase boundary. This point is reinterpreted as the S-CAF (S–FCAF) phase transition point due to the fact that the S-CAF region seems to vanish at σ=0 in the present work. We also plot these two points as solid diamonds in Fig. 7. The S-CAF phase boundary of the current data is slightly different from the one determined from Ref. 21. One reason of this discrepancy of the S-CAF phase boundary is the method to determine the phase boundary. To analyze the S-CAF phase transition point in Ref. 21, we need the assumption that the SCAF phase vanishes at σ=0, and thus the FCAF-SCAF phase boundary coincides to the S-FCAF phase boundary. Another possibility is different measuring methods. Though the Hall plateau width measurements and the activation energy measurements present qualitatively similar results, there is no reason that these two results are identical. The activation energy measurement is more reliable.

VI. COMMENTS

Carrying out elaborate magnetotransport measurements, we have established the existence of three phases in the ν=2 bilayer QH system. Our new finding is an intrinsic structure of the CAF phase represented by the FCAF and SCAF regions in the imbalanced density configuration.

We make comments on related theoretical works. Brey *et al.* predicted that there arise new coherent phases for large layer density imbalance.[16] For large bias voltage the CAF phase would become the coherent canted (CC) phase. However this CC phase is only stable at zero tunneling limit Δ_{SAS}=0. Since our sample has a large tunneling energy, it is difficult to identify the region IV as the CC phase. Demler *et al.* suggested that there exist the Bose-glass phase due to nonzero disorder effect.[11] Though their theoretical calculation was performed only in the balanced density configuration, it would be worthwhile to try to identify the region II

京都大学 KYOTO UNIVERSITY
A Self-archived copy in
Kyoto University Research Information Repository
https://repository.kulib.kyoto-u.ac.jp
京都大学学術情報リポジトリ KURENAI 紅 Kyoto University Research Information Repository

(IV) with a Bose-glass phase made of domains of the CAF phase surrounded by domains of the F (S) phase. However, a theoretical study of the Bose-glass phase in the imbalanced configuration will be indispensable for further discussions.

ACKNOWLEDGMENTS

We are grateful to T. Saku for growing the heterostructures, and K. Muraki for fruitful discussions. We also thank T. Nakajima for much fruitful advice for theoretical calculations. This research was supported in part by Grants-in-Aid for the Scientific Research and Technology of Japan (Grant Nos. 14010839, 14340088) and a 21st Century COE Program Grant of the International COE of Exploring New Science Bridging Particle-Matter Hierarchy from the Ministry of Education, Culture, Sports, Science. A part of this work was performed at the clean room facility of the Center for Interdisciplinary Research of Tohoku University.

*Electronic address: fukuda@scphys.kyoto-u.ac.jp

[1] A. P. Mackenzie and Y. Maeno, Rev. Mod. Phys. **75**, 657 (2003).
[2] A. Görlitz *et al.*, Phys. Rev. Lett. **87**, 130402 (2001).
[3] V. Schweikhard, I. Coddington, P. Engels, V. P. Mogendorff, and E. A. Cornell, Phys. Rev. Lett. **92**, 040404 (2004).
[4] J. C. Davis, A. Amar, J. P. Pekola, and R. E. Packard, Phys. Rev. Lett. **60**, 302 (1988).
[5] *Perspectives in Quantum Hall Effects*, edited by A. Pinczuk and S. Das Sarma (Wiley, New York, 1997).
[6] Z. F. Ezawa, *Quantum Hall Effects, Field Theoretical Approach and Related Topics* (World Scientific, Singapore, 2000).
[7] L. Zheng, R. Radtke, and S. Das Sarma, Phys. Rev. Lett. **78**, 2453 (1997).
[8] S. Das Sarma, S. Sachdev, and L. Zheng, Phys. Rev. Lett. **79**, 917 (1997); Phys. Rev. B **58**, 4672 (1998).
[9] V. Pellegrini, A. Pinczuk, B. S. Dennis, A. S. Plaut, L. N. Pfeiffer, and K. W. West, Phys. Rev. Lett. **78**, 310 (1997).
[10] V. Pellegrini, A. Pinczuk, B. S. Dennis, A. S. Plaut, L. N. Pfeiffer, and K. W. West, Science **281**, 799 (1998).
[11] E. Demler and S. Das Sarma, Phys. Rev. Lett. **82**, 3895 (1999).
[12] K. Yang, Phys. Rev. B **60**, 15 578 (1999).
[13] Y. Shimoda, T. Nakajima, and A. Sawada, Physica E (Amsterdam) **22**, 56 (2004); Int. J. Mod. Phys. B (to be published); Mod. Phys. Lett. B (to be published).
[14] J. Schliemann and A. H. MacDonald, Phys. Rev. Lett. **84**, 4437 (2000).
[15] A. H. MacDonald, R. Rajaraman, and T. Jungwirth, Phys. Rev. B **60**, 8817 (1999).
[16] L. Brey, E. Demler, and S. Das Sarma, Phys. Rev. Lett. **83**, 168 (1999).
[17] Z. F. Ezawa, M. Eliashvili, and G. Tsitsishvili, Phys. Rev. B **83**, 168 (2005).
[18] V. S. Khrapai, E. V. Deviatov, A. A. Shashkin, V. T. Dolgopolov, F. Hastreiter, A. Wixforth, K. L. Campman, and A. C. Gossard, Phys. Rev. Lett. **84**, 725 (2000).
[19] A. Sawada, Z. F. Ezawa, H. Ohno, Y. Horikoshi, Y. Ohno, S. Kishimoto, F. Matsukura, M. Yasumoto, and A. Urayama, Phys. Rev. Lett. **80**, 4534 (1998).
[20] A. Sawada, Z. F. Ezawa, H. Ohno, Y. Horikoshi, A. Urayama, Y. Ohno, S. Kishimoto, F. Matsukura, and N. Kumada, Phys. Rev. B **59**, 14 888 (1999).
[21] N. Kumada, D. Terasawa, M. Morino, K. Tagashira, A. Sawada, Z. F. Ezawa, K. Muraki, Y. Hirayama, and T. Saku, Phys. Rev. B **69**, 155319 (2004).
[22] S. J. Geer, A. G. Davies, C. H. W. Barnes, K. R. Zolleis, M. Y. Simmons, and D. A. Ritchie, Phys. Rev. B **66**, 045318 (2002).
[23] K. Muraki, N. Kumada, T. Saku, and Y. Hirayama, Jpn. J. Appl. Phys., Part 1 **39**, 2444 (2000).